Journal of Engineering Sciences, Assiut University, Vol. 34, No. 3, pp. 779-797, May 2006

ROBUST CONTROL BASED ON H$_\infty$ APPROACH FOR A WIND DRIVEN INDUCTION GENERATOR CONNECTED TO THE UTILITY GRID

A. A. Hassan* **;** ***Yehia S. Mohamed***
Electrical Engineering Department, Faculty of Engineering , El -Minia University, Egypt

Ali M. Yousef **** ***and A. M. Kassem***
Electrical Engineering Department, Faculty of Engineering, Assiut University, Egypt
* aahsn@yahoo.com
** Alimy1@yahoo.com

(Received January 16, 2006 Accepted February 18, 2006)

ABSTRACT– *This paper proposes the application of H$_\infty$ synthesis to design a robust controller for regulating the voltage and frequency of a wind generation system. The controlled system consists of a wind turbine that drives an induction generator connected to the utility grid through asynchronous AC-DC-AC link. The main control objective is to regulate the DC link voltage and to track and extract maximum available wind power. This is accomplished via controlling the firing angles of the rectifier and the inverter. The complete nonlinear dynamic model of the system has been described and linearized around an operating point. Also, the design problem of the H$_\infty$ controller has been formulated in a standard form with emphasis on the selection of the weighting functions that reflect robustness and performance goals. The proposed system has the advantages of robustness against model uncertainties and external disturbances, fast response and the ability to reject noise. The performance of the wind generation system with the proposed controller has been tested through a step and sinusoidal changes in reference input power. In addition, detuned system parameters are assumed. Simulation results confirm that good dynamic performance of the proposed wind energy scheme has been achieved.*

KEYWORDS: *wind turbine - induction generator - H infinity - robust control.*

NOMENCLATURE

v_{ds}, v_{qs}	d-q stator voltages,
i_{ds}, i_{qs}	d-q stator currents,
i_{dr}, i_{qr}	d-q rotor currents,

R_s , R_r	stator and rotor resistances per phase,
L_s , L_r , L_m	stator, rotor and magnetizing inductances
C_0	self excitation capacitance per phase
ω_s	Angular stator frequency of the induction generator
ω_m	Angular rotor speed (electrical rads/s) of the induction generator
J	moment of inertia
f	friction coefficient
p	differential operator *d/dt*
L_{DC}	DC-link inductance
R_{DC}	DC-link resistance
α_R , α_I	firing angles of the converter and inverter.
v_{dcon} , v_{qcon}	d-q input voltage of the converter.
i_{dcon} , i_{qcon}	d-q input current of the converter.
I_{DC}	DC-link current.
v_{inv}	inverter output voltage
P	number of pole pairs

1. INTRODUCTION

Nowadays, the wind energy has gained a lot of attention and became one of the most promising renewable resources. The squirrel cage induction machine is ideally suited for use in wind energy applications as it requires low maintenance, and is built robustly to withstand severe operating conditions [1]. One of the simplest methods of running a wind generation system is to use an induction generator connected directly to the utility grid. This is a very common method of operation which force the machine to run at a constant frequency and therefore at nearly constant speed. Because the wind is highly variable, it is very desirable to operate a wind turbine at variable speeds [2]. In this case, a large fraction of the available wind energy can be extracted by maintaining the optimal tip speed ratio.

Various control strategies have been proposed for regulating grid voltage and / or achieving optimal output power of the turbine. In some schemes, the wind turbine drives an induction generator connected to grid through a static converter [2-3]. Other control schemes use search methods that vary the speed until optimal power is obtained [4-5]. However, these techniques have the difficulty of tracking the wind which will cause additional stress on the shaft.

Recently, advanced control tehniques, which were applied successfully on the machine drives, have been proposed for regulating the wind power in a grid connected wind energy conversion scheme. In the first approach [6], the dead beat control of output power was proposed. However, the knowledge of wind speed must be necessary for controller implementation. In other approaches [7-8], the sliding mode technique has been employed in a variable structure controller for regulating the output power. The proposed sliding mode controller has the advantages of robustness against parameter uncertainties as well as wind disturbances. However, an inevitable chattering resulting from the switching of the control structure still exist. Moreover, the wind estimation would be needed in [7] while a speed sensor must be existed in [8] to measure the rotor speed.

In [9], a fuzzy logic based intelligent controller has been used extensively to optimize efficiency and enhance performance of a variable speed wind generation system. This controller has the advantages that it does not require the mathematical model of the system besides the insensitivity to external disturbance and erroneous information. However, this system has two drawbacks. First, the operating point oscillates largely with the change in wind speed. Second, a speed sensor is needed to provide the speed signal.

The linear quadratic Gaussian controller has been applied [10-11] to regulate the terminal voltage, and optimize the power output of a wind energy conversion scheme. The merits of this controller are summarized as: fast response, robustness, and the ability to operate with available noise data. On the other hand, this controller has the demerits that it needs an accurate system model, no stability margin is guaranteed and more computational effort is required.

During the past decade, the H_∞ control theory has been widely celebrated for its robustness in counteracting uncertainty perturbations and external disturbances. As a consequence, some applications of this approach to various plants such as dc motors [12], switching converters [13], synchronous motors [14], induction motors [15], have been published. The main point of the H_∞ control is to synthesize a feedback law that renders the closed loop system to satisfy a prescribed H_∞ - norm constraint. This would satisfy the desired stability and the tracking requirements.

This paper presents the voltage and frequency control of a wind driven induction generator connected to the utility grid via an asynchronous AC-DC-AC link. The H_∞ optimal controller has been employed to regulate the DC voltage at the rectifier output and track maximum available wind power. This is achieved by controlling the firing angles of the converter and inverter respectively. The terminal voltage and power at the rectifier output are measured and used as feedback signals. The linearized mathematical model of the proposed wind energy system has been described. Also, the formulation and design of the H_∞ controller have been given. The proposed control strategy has several attractive features such as robust stability against system uncertainties, disturbances, and measurment noises. Moreover, it has simple implementation, and low computational burden. Furthermore, it does not need either the wind speed estimation or the knowledge of turbine aerodynamics like other control methods.

The feasibility and effectiveness of the wind energy generating scheme together with the proposed H_∞ controller have been demonstrated through computer simulations. Simulation results have proved that the proposed controller can give better overall performance.

2. SYSTEM DESCRIPTION

Figure 1 shows a wind energy system connected to the utility grid via an asynchronous AC-DC-AC link. It consists of a vertical axis wind turbine, driving a self excited induction generator. The asynchronous link consists of a six pulse line commutated converter, a smoothing reactor, and a six pulse line commutated inverter. This system essentially converts the variable voltage variable frequency voltage at the induction generator terminals to constant voltage constant frequency at the grid terminals. The DC link decouples the induction generator and the utility systems such that each system operates at its own frequency. This enables the induction generator to operate over a wide speed range. The flow of power across the DC link can be controlled by adjusting the firing angles of the controlled rectifier and the inverter.

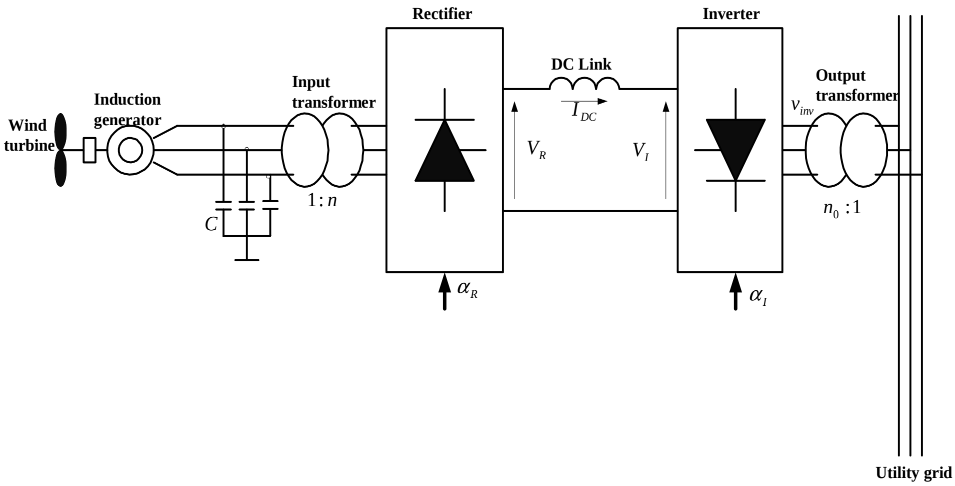

Fig. 1: Schematic diagram of the proposed wind energy system.

3. SMALL SIGNAL LINEARIZED MODEL

The nonlinear dynamic model of the wind generation system can be desribed by the following nine differential equations (1-9) (the proof is found in appendix A)[16] :

$$pi_{qs} = -R_s A_1 i_{qs} - \left(\frac{i_{qs} + \frac{2\sqrt{3}}{\pi} nI_{DC} \sin\alpha_R}{C_0 v_{ds}} + A_2\omega_m L_m\right) i_{ds} + R_r A_2 i_{qr} - A_1\omega_m L_r i_{dr} \quad (1)$$

$$pi_{ds} = \left(\frac{i_{qs} + \frac{2\sqrt{3}}{\pi} nI_{DC} \sin\alpha_R}{C_0 v_{ds}} + A_2\omega_m L_m\right) i_{qs} - R_s A_1 i_{ds} + R_r A_2 i_{dr} + A_1\omega_m L_m i_{qr} - A_1 v_{ds} \quad (2)$$

$$pi_{qr} = R_s A_2 i_{qs} + A_2\omega_m L_s i_{ds} - A_3 i_{qr} + \left(-\frac{i_{qs} + \frac{2\sqrt{3}}{\pi} nI_{DC} \sin\alpha_R}{C_0 v_{ds}} + A_1\omega_m L_s\right) i_{dr} \quad (3)$$

$$pi_{dr} = -A_2\omega_m L_s i_{qs} + R_s A_2 i_{ds} + \left(\frac{i_{qs} + \frac{2\sqrt{3}}{\pi} nI_{DC}\sin\alpha_R}{C_0 v_{ds}} - A_1\omega_m L_s\right)i_{qr} - A_3 i_{dr} + A_2 v_{ds} \quad (4)$$

$$p\omega_m = (-f\omega_m + PT_m + 1.5P^2 L_m(i_{qs}i_{dr} - i_{ds}i_{qr}))/J \quad (5)$$

$$pv_{ds} = \frac{i_{ds} - \frac{2\sqrt{3}}{\pi} nI_{DC}\cos\alpha_R}{C_0} \quad (6)$$

$$pI_{DC} = \left(-R_{DC}I_{DC} + \frac{3\sqrt{3}}{\pi} nv_{ds}\cos\alpha_R + \frac{3\sqrt{3}}{\pi} v_{inv}\cos\alpha_I - \frac{3x_{ci}}{\pi} I_{DC}\right)/L_{DC} \quad (7)$$

$$p\alpha_R = V_{ref} - V_R = V_{ref} - \frac{3\sqrt{3}}{\pi} nv_{ds}\cos\alpha_R \quad (8)$$

$$p\alpha_I = P_{ref} - P = P_{ref} - \left(\frac{3\sqrt{3}}{\pi} nv_{ds}\cos\alpha_R\right)I_{DC} \quad (9)$$

The H∞ controller proposed for regulating the voltage and power output of the system under study is based on the state space linear model. Therefore, the nonlinear dynamic model of the complete wind energy conversion system is linearized arround an operating point. The linearized model takes the following state matrix form :

$$px = Ax + Bu, \qquad y = Cx$$

where $x = [\Delta i_{qs} \quad \Delta i_{ds} \quad \Delta i_{qr} \quad \Delta i_{dr} \quad \Delta\omega_s \quad \Delta v_{ds} \quad \Delta I_{DC} \quad \Delta\alpha_R \quad \Delta\alpha_I]^T$,

$u = [\Delta V \quad \Delta P]^T$, $B = \begin{bmatrix} 0 & 0 & 0 & 0 & 1 & 0 \\ 0 & 0 & 0 & 0 & 0 & 1 \end{bmatrix}^T$, and

A = $[a_{ij}]$ is a 9 x 9 matrix containing the system parameters. The elements a_{ij} are written in appendix (B), $\Delta V = V_{ref} - V_R$ is the difference between the reference and actual rectifier output voltage.

$\Delta P = P_{ref} - P$ is the difference between the reference and actual rectifier output power.

4. H∞ CONTROLLER DESIGN

The H∞ theory provides a direct, reliable procedure for synthesizing a controller which optimally satisfies singular value loop shaping specifications [17]. The standard setup of the H∞ control problem consists of finding a static or dynamic feedback controller such that the H∞ norm (a standard quantitative measure for the size of the system uncertainty) of the closed loop transfer function is less than a given positive number under constraint that the closed loop system is internally stable.

The H_∞ synthesis is carried out in two stages:

i. Formulation: weighting the appropriate input-output transfer functions with proper weighting functions. This would provide robustness to modeling errors and achieve the performance requirements. The weights and the dynamic model of the system are then augmented into H_∞ standard plant.

ii. Solution: the weights are iteratively modified until an optimal controller that satisfies the H_∞ optimization problem is found.

Figure 2 shows the general setup of the H_∞ design problem where :

P(s) is the transfer function of the augmented plant (nominal plant G(s) plus the weighting functions that reflect the design specifications and goals).

u2 is the exogenous input vector, typically consists of command signals, disturbance, and measurement noises,

u1 is the control signal,

y2 is the output to be controlled, its components typically being tracking errors, filtered actuator signals,

y1 is the measured output.

The objective is to design a controller F(s) for the augmented plant P(s) such that the input/output transfer characteristics from the external input vector u2 to the external output vector y2 is desirable. The H_∞ design problem can be formulated as finding a stabilizing feedback control law u1 (s) = F(s) . y1(s) such that the norm of the closed loop transfer function is minimized.

In the proposed wind generation system including H_∞ controller, two feedback loops are designed; one for adjusting the terminal voltage and the other for regulating the output power as shown in **Fig. 3**. The nominal system G(s) is augmented with weighting transfer functions $W_1(s)$, $W_2(s)$ and $W_3(s)$ penalizing the error signals, control signals, and output signals respectively. The choice of proper weighting functions is the essence of H_∞ control. A bad choice of weights will certainly lead to a system with poor performance and stability characteristics, and can even prevent the existence of a solution to the H_∞ problem.

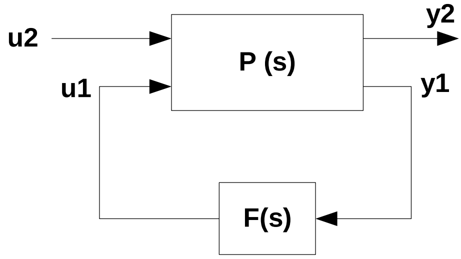

Figure 2: General setup of the H_∞ design problem

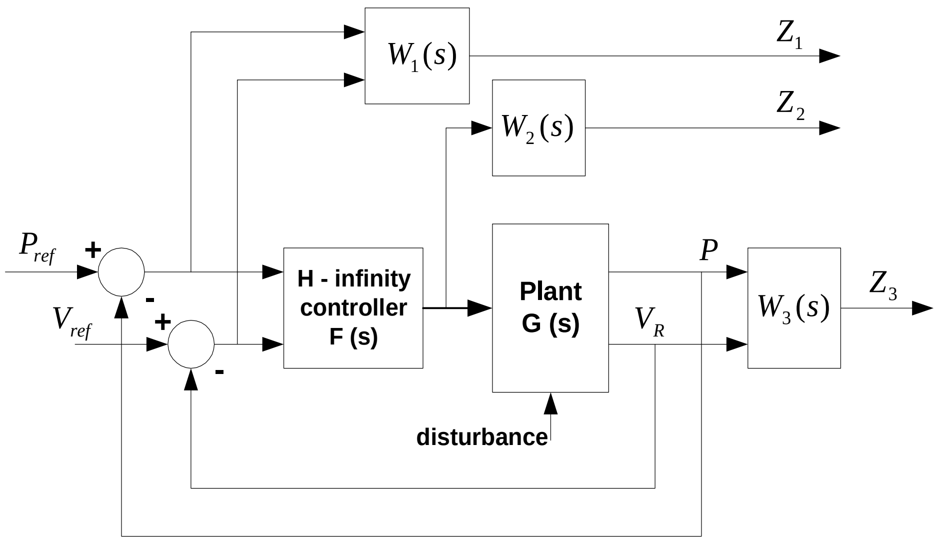

Figure 3: Simplified block diagram of the augmented plant including H∞ controller.

Consider the augmented system shown in Fig. (3). The following set of weighting transfer functions are chosen to reflect desired robust and performance goals as follows:

A good choice of $W_1(s)$ is helpful for achieving good tracking of the input references, and good rejecting of the disturbances. The weighted error transfer function matrix Z_1 ; which is required to regulate, can be written as :

$$Z_1 = W_1(s)\begin{bmatrix} V_{ref} - V_R \\ P_{ref} - P \end{bmatrix}$$

A good choice of the second weight $W_2(s)$ will aid for avoiding actuators saturation and provide robustness to plant additive perturbations. The weighted control function matrix Z_2 can be written as :

$$Z_2 = W_2(s).\,u(s)$$

where $u(s)$ is the transfer function matrix of the control signals output of the H∞ controller.

Also a good choice of the third weight $W_3(s)$ will limit the closed loop bandwidth and achieve robustness to plant output multiplicative perturbations and sensor noise attenuation at high frequencies. The weighted output variable can be written as:

$$Z_3 = W_3(s) \begin{bmatrix} V_R \\ P \end{bmatrix}$$

In summary, the transfer functions of interest which determine the behavior of the voltage and power closed loop systems are:

a) Sensitivity function : $S = [I + G(s) . F(s)]^{-1}$

Where G(s) and F(s) are the transfer functions of the nominal plant and the H_∞ controller respectively, and I is the identity matrix. Minimizing S at low frequencies will insure good tracking and disturbance rejection.

b) Control function : $C = F(s) [I + G(s) . F(s)]^{-1}$

Minimizing C will avoid actuator saturation and achieve robustness to plant additive perturbations.

c) Complementary function : $T = I - S$

Minimizing T at high frequencies will insure robustness to plant output multiplicative perturbations and achieve noise attenuation.

5. IMPLEMENTATION SCHEME

The main objectives of the proposed controller are :

i) Tracking maximum available wind power (to fully utilize the available wind energy) at any given wind speed, and
ii) Minimizing the reactive power consumed by the converter, so as to optimize the size and capacity (VARs) of the self excitation capacitor bank connected at the terminals of the induction machine.

For this purpose, the controlled system has been designed to contain two feedback loops. The first loop is designed for adjusting the induction generator terminal voltage at the rectifier output according to a certain reference. The other loop has been dedicated for regulating the output power to a set point, thereby, maximum available wind power can be tracked at any given wind speed.

The block diagram of the wind energy conversion system with the proposed H_∞ controller is shown in Fig. (4). The entire system has been simulated on the digital computer using the Matlab / Simulink software package. The specifications of the system used in the simulation procedure are listed in appendix (C)[16]. The following set of weighting functions are chosen after many iterations in order to achieve the desired robustness and performance goals:

$$W_1 = \begin{bmatrix} \gamma_{11}\dfrac{s+50}{s+70} & 0 \\ 0 & \gamma_{12}\dfrac{s+1500}{s+600} \end{bmatrix}, \qquad W_2 = \begin{bmatrix} \gamma_{21}\dfrac{s+30}{s+666} & 0 \\ 0 & \gamma_{22}\dfrac{s+3}{s+40} \end{bmatrix} \quad \text{and}$$

$$W_3 = \begin{bmatrix} \gamma_{31}\dfrac{s+0.0374}{s+900} & 0 \\ 0 & \gamma_{32}\dfrac{s+0.00465}{s+1500} \end{bmatrix}$$

Where

$\gamma_{11} = 0.0005$, $\gamma_{12} = 0.001$, $\gamma_{21} = 0.012$, $\gamma_{22} = 0.02$, $\gamma_{31} = 0.1712$, $\gamma_{32} = 0.43$.

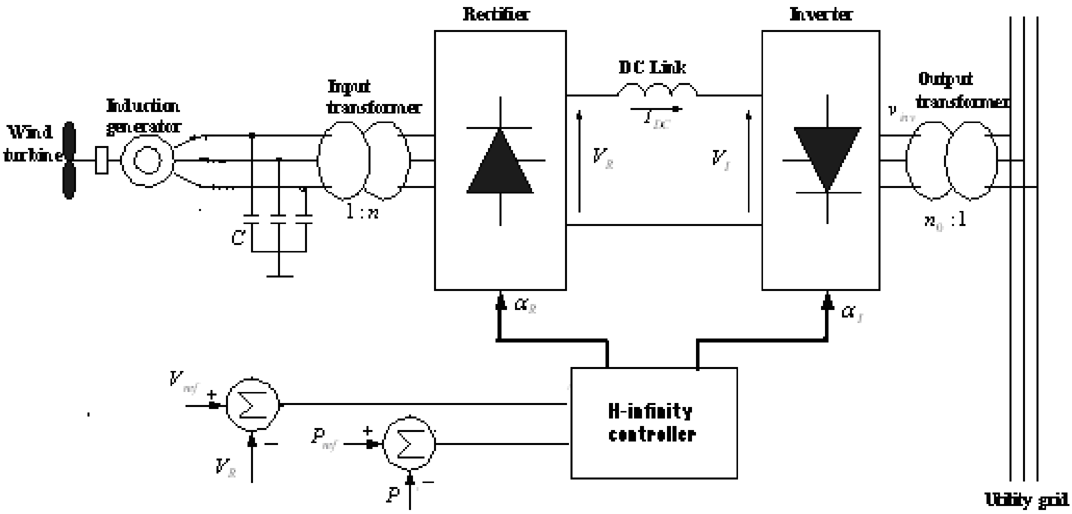

Fig. 4: Block diagram of the wind energy conversion system with the proposed H∞ controller.

6. RESULTS

Computer simulations have been carried out in order to validate the effectiveness of the proposed scheme. At first, the eigen values of the system under study are examined; for the purpose of comparison, with and without the H∞ controller as shown in **Table 1**. It is seen that the open loop system is unstable at the chosen operating point while all the poles of the augmented system including the H∞ controller has negative real parts in the complex s – plane. Moreover, these poles has damping ratios between 0.133 to 1. This will ensure the damping performance of the closed loop system.

Table 1: Eigen values of the system under study with and without the H∞ controller.

Without H∞ controller (open loop system)	**With H∞ controller (augmented system)**
-62.232 ± 374.53i	-62.232 ± 374.53i , -44.748 ± 332.75i
65.312 ± 317.32i	-68.418 ± 316.88i , -125.94 ± 275.53i
-207.62	-45.198 ± 5.6002i
187.92	-909.12 , -737.54 , -599.87 , -207.62 ,
-20.365	-194.14 , -146.93 , -69.998 , -21.499 ,
16.626	-20.365 , -17.545 , -5.0122 , -3.3215 ,
0.82602	-0.82612 , -1604.8 , -600 , -666.27 ,
	-40 , -70 , -1500 , -900 .

The performance of the proposed system has been tested with a step change in wind speed. Thus, the wind speed is assumed to vary abruptly from 6.4 m/sec. to 6.5 m/sec. at t = 2 seconds. This means that the power reference increases from 165 to 173 watts. Also, the system parameters are assumed to have detuned values through the simulation. Thus, the parameters of the induction generator deviate from their nominal values by + 50% in the stator and rotor resistances, +20% in the stator and rotor leakage inductances, -10% in the magnetizing inductance, and +50% in the moment of inertia and friction coefficient. Moreover, the parameters of the dc link are permitted to deviate by +50% in its resistance, and +200% in the inductance. **Figure 5** illustrates the dynamic responses of the d-q stator current components and rotor speed of the induction generator, firing angles for both rectifier and inverter, reference and actual rectifier output voltages, reference and actual rectifier output powers, and DC link current. Simulation waveforms may be interpretted as follows:

a) The step change in reference power will cause the power error to increase, consequently, the inverter firing angle will increase also (Eqn 9). This is in turn will increase the inverter input voltage. On the hand, the dc link current decreases slightly as a result of the positive change of inverter firing angle keeping in mind that the rectifier output voltage hasn't been changed yet. The decrement of dc link current will imply that the rectifier input current to decrease also. This in turn will

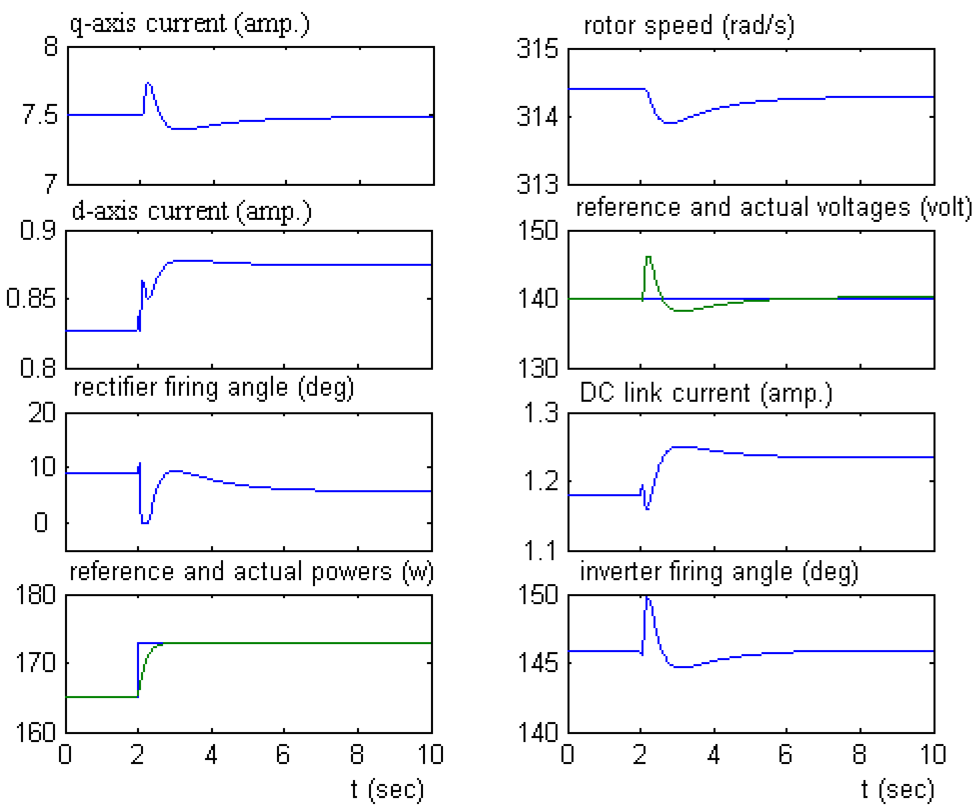

Fig. 5: Dynamic responses of the proposed scheme to a step change in wind speed.

require that the terminal voltage of the induction generator rises and so the rectifier output voltage. Therefore, the firing angle of the rectifier will be decreased to satisfy the requirement of the voltage increment.

b) As the voltage error increases, the closed loop adjusts the rectifier voltage causing the firing angle to increase untill this error disappears.
c) The power closed loop adjusts the inverter firing angle untill the actual power is equal to the reference one. The dc link current increases to satisfy the power requirement.
d) As a result of providing more power to the grid, the load on the induction generator increases. This would affect the rotor speed dynamic response slightly.

It has been noticed in the figure that the actual converter output power tracks accurately the reference one with small steady state error equal to about 0.03 % , and less than 1 sec. rise time. On the other hand, an overshoot with amplitude equal to 4.2 % has been noticed in the response of the actual voltage output from the rectifier, but it dies fastly. The figure reports also that the steady state error between the actual and reference voltages is equal to about 0.15 %. It is worthy to note that, reducing the voltage overshoot is possible by modifying the weights but at the expense of increasing the steady state error.

The wind generation system with the proposed H_∞ controller has been tested also with sinusoidal variation of wind speed. Thus, the wind speed is assumed to vary sinusoidally from 6.077 m/sec. to 6.277 m./sec. with an average equal to 6.177 m./sec. This corresponds to reference power variation from 157.2 to 173.2 watts. The frequency of the wind speed variation is assumed to be equal to 12 cycles per minute. The system parameters are detuned as in the previous case. **Figure 6** illustrates the dynamic responses of the proposed system under the influence of such variation. The following points are concluded:

a) The rotor speed of the induction generator oscillates in response to the wind speed variation.
b) Good tracking between the reference and actual powers is evident.
c) A small deviation of the actual voltage around its reference (about ± 0.36 %) has been reported.
d) The rectifier firing angle oscillates between 5 and 12.6° in order to regulate the voltage.
e) The inverter firing angle swings between 146.1 and 146.5° in order to keep tracking of the actual power.
f) The stator current components and the dc link current oscillate about their average values to meet the control requirements.

7. CONCLUSIONS

In this paper, the H_∞ control theory has been used in order to design a state feedback static controller for a wind driven generation system. The controlled system consists of a wind turbine that drives an induction generator connected to the utility grid through asynchronous AC-DC-AC link. The control objective aims to regulate the rectifier

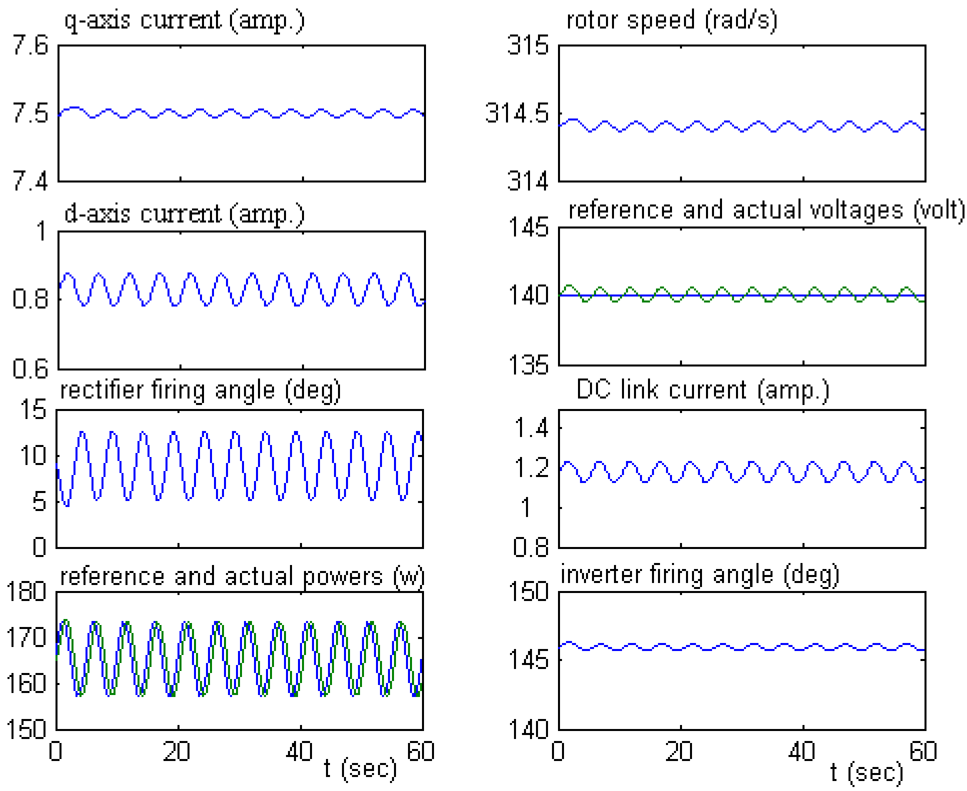

Fig. 6: Dynamic response of the proposed scheme to sinusoidal variation of wind speed.

output voltage at maximum available wind power. This is carried out via controlling the firing angles of both the rectifier and the inverter. The complete dynamic model of the system has been described and linearized around a working point. The design problem of the H_∞ controller has been described and formulated in the standard form with emphasis on the selection of weighting functions that satisfy optimal robustness and performance. The proposed control strategy has many advantages like robustness to plant uncertainities, simple implementation, and fast response.

The stability and tracking performance of the proposed system including mismatched parameters have been evaluated through step and sinusoidal variations of input power reference. The results proved that good dynamic performance, and high robustness in face of uncertainities can be achieved by means of the proposed controller.

REFERENCES

[1] L. J. Bohmann, D. O. Wlltanen, and A. Bose " A variable voltage and frequency scheme to optimize the efficiency of a wind driven induction generator", Electric Machines and Power Systems, Vol. 24, 1996, pp 429-435.

[2] A. Miller, E. Muljadi and D. S. Zinger, " A variable speed wind turbine power control", IEEE Trans. On Energy Conversion, Vol. 12, No. 2, June, 1997, pp 181-186.

[3] A. Abdin and X. Wilson, " Control design and dynamic performance analysis of a wind turbine-induction generator unit", IEEE Trans. On Energy Conversion, Vol. 15, No. 1, March, 2000, pp 91-96.

[4] R. Spee, S. Bhowmik and J. H. R Enslin, " Adaptive control strategies for variable-speed doubly-fed wind power generation systems", IAS Annual meeting, October, 1995, pp 545-552.

[5] M. G. Simoes, B. K. Bose and R. J. Spiegel, "Fuzzy logic based intelligent control of a variable speed cage machine wind generation system", PFSC, 1995, pp 389-395.

[6] T. Thiringer and J. Linders, " Control by variable rotor speed of fixed pitch wind turbine operating in speed range", IEEE Trans. On Energy Conversion, Vol. 8, Sept. 1993, pp 520 - 526.

[7] H. De Battista, R. J. Mantz and C. Christiansen, "Dynamical sliding mode power control of wind driven induction generators", IEEE Trans. On Energy Conversion, Vol. 15, December 2000, pp 451-457.

[8] H. De Battista and R. J. Mantz "Dynamical variable stracture controller for power regulation of wind energy conversion systems", IEEE Trans. On Energy Conversion, Vol. 19, No. 4, December 2004, pp 756-763.

[9] M. Godoy, B. K. Bose and R. J. Spiegel, "design and performance evaluation of a fuzzy-logic-based variable-speed wind generation system", IEEE Trans. On Energy Conversion, Vol. 33, no. 4, July 1997, pp 956-964.

[10] I. Munteau, N. A. Cutululis, A. I. Bratcu, and E. Ceanga, " Optimization of variable speed wind power systems based on a LQG approach", IFAC workshop on Control Applications of Optimisation - CAO'03 Visegrad, Hungary, June / July 2003.

[11] A. A. Hassan, Y. S. Mohamed, A. M. Yousef, and A. M. Kassem," Robust control of a wind driven induction generator connected to the utility grid", Accepted, and will be published in the Bulletin of the Faculty of Engineering, Assiut University, Jan. 2006.

[12] C. Attaiaence, A. Perfetto, and G. Tomasso, "Robust postion control of DC drives by means of H_∞ controllers ", Proc. IEE – Elect. Power Applications, Vol. 146, No. 4, 1999, pp. 391-396.

[13] R. Naim, G. Weiss, and S. Ben-Yakakov," H_∞ control applied to boost power converters", IEEE Trans. Power Electronics, Vol. 12, July 1997, pp 677- 683.

[14] Faa-Jeng Lin, T. Lee, and C. Lin, " Robust H_∞ controller design with recurrent neural network for linear synchronous motor drive", IEEE Trans. On Industrial Electronics, Vol. 50, No. 3, June 2003, pp 456 - 470.

[15] C. Attaianese, and G. Tomasso, " H_∞ controller design and implementation for induction motors ", T. IEE Japan, Vol. 121 – D, No. 6, 2001, pp. 635 - 641.

[16] R. M. Hilloowala, “ Control and interface of renewable energy systems”, Ph.D. Thesis, The University of New Brunswick, Canada, 1992.

[17] R. Y. Chiang, and M. G. Safonov," Robust Control Toolbox Matlab User’s Guide".

APPENDIX A : COMPLETE SYSTEM MODEL

The mathematical models of the different parts of the wind generation system are described as follows**:**

A.1 Wind Turbine Dynamic Model

The wind turbine is characterized by nondimensional curves of the power coefficient C_p as a function of both the tip speed ratio, λ and the blade pitch angle, β. In order to fully utilize the available wind energy, the value of λ should be maintained at its optimum value. Hence, the power coefficient corresponding to that value will become maximum also.

The tip speed ratio λ can be defined as the ratio of the angular rotor speed of the wind turbine to the linear wind speed at the tip of the blades. It can be expressed as follows:

$$\lambda = \omega_t R / V_w \tag{a1}$$

Where R is the wind turbine rotor radius, V_w is the wind speed and ω_t is the mechanical angular rotor speed of the wind turbine.

The output power of the wind turbine, can be calculated from the following equation

$$P_m = 0.5 \rho A C_p V_w^3 \tag{a 2}$$

Where ρ is the air density, and A is the swept area by the blades.

Also, the torque available from the wind turbine can be expressed as :

$$T_m = 0.5 \rho A R C_p V_w^2 / \lambda \tag{a 3}$$

A.2 Induction Generator Dynamic Model

The dynamic behavior of the induction generator in the d-q axis synchronously rotating reference frame is given by [16]:

$$pi_{qs} = -R_s A_1 i_{qs} - (\omega_s + A_2 \omega_m L_m) i_{ds} + R_r A_2 i_{qr} - A_1 \omega_m L_r i_{dr} \tag{a 4}$$

$$pi_{ds} = (\omega_s + A_2 \omega_m L_m) i_{qs} - R_s A_1 i_{ds} + R_r A_2 i_{dr} + A_1 \omega_m L_m i_{qr} - A_1 v_{ds} \tag{a 5}$$

$$pi_{qr} = R_s A_2 i_{qs} + A_2 \omega_m L_s i_{ds} - A_3 i_{qr} + (-\omega_s + A_1 \omega_m L_s) i_{dr} \tag{a 6}$$

$$pi_{dr} = -A_2 \omega_m L_s i_{qs} + R_s A_2 i_{ds} + (\omega_s - A_1 \omega_m L_s) i_{qr} - A_3 i_{dr} + A_2 v_{ds} \tag{a 7}$$

Where $v_{qs} = 0$, due to the choice of axis alignment, and

$A_1 = L_r / (L_s L_r - L_m^2)$, $A_2 = L_m / (L_s L_r - L_m^2)$, and $A_3 = R_r (1 + A_2 L_m) / L_r$

The rotor speed ω_m is governed by the following differential equation :

$$T_m + T_e = (Jp + f) \omega_m / P \tag{a 8}$$

Where T_m is the input torque from the prim-mover, and T_e is the electromagnetic torque representing the load on the induction generator (T_e is negative for generator action) which is given by:

$$T_e = 1.5PL_m(i_{qs}i_{dr} - i_{ds}i_{qr}) \quad \text{(a 9)}$$

Equations (8) and (9) are combined as

$$p\omega_m = (-f\omega_m + PT_m + 1.5P^2L_m(i_{qs}i_{dr} - i_{ds}i_{qr}))/J \quad \text{(a 10)}$$

A.3 Asynchronous DC Link Model

The asynchronous DC link (used to interface the wind energy system to the utility) consists of a six pulse line commutated converter, a smoothing reactor, and a six pulse line commutated inverter. An isolating transformer of turns ratio $1:n$ interconnects the induction generator to the converter. Neglecting the resistance and leakage reactance of the isolating transformer, the various ac quantities on the primary and secondary sides can be related by:

$$v_{dcon} = nv_{ds} \;,\quad v_{qcon} = nv_{qs} \;,\quad i_{qcon} = i_{ql}/n \;,\quad i_{dcon} = i_{dl}/n \quad \text{(a 11)}$$

Assuming the converter is lossless, the instantaneous power balance equation ($v_{qcon} = 0$, due to the choice of axis alignment):

$$\frac{3}{2}v_{dcon}i_{dcon} = V_R I_{DC} \quad \text{(a 12)}$$

Where V_R is the DC voltage at the converter output terminals which can be written as :

$$V_R = \frac{3\sqrt{3}}{\pi} nv_{ds}\cos\alpha_R \quad \text{(a 13)}$$

The ac and dc currents of the converter are related by :

$$i_{con} = \sqrt{(i_{qcon}^2 + i_{dcon}^2)} = \frac{2\sqrt{3}}{\pi} I_{DC} \quad \text{(a 14)}$$

Neglecting the commutation overlap, the d-q converter currents can be deduced using equations (a 12-a 14) as:

$$i_{dcon} = i_{con}\cos\alpha_R = \frac{2\sqrt{3}}{\pi} I_{DC}\cos\alpha_R \quad \text{(a 15)}$$

$$i_{qcon} = -i_{con}\sin\alpha_R = -\frac{2\sqrt{3}}{\pi} I_{DC}\sin\alpha_R \quad \text{(a 16)}$$

Referring to Fig. (1), the dynamics introduced by the DC link is given by:

$$L_{DC}pI_{DC} + R_{DC}I_{DC} = V_R - V_I \quad \text{(a 17)}$$

Where V_I is the DC voltage at the inverter input terminals which can be expressed as :

$$V_I = -\frac{3\sqrt{3}}{\pi} v_{inv} \cos\alpha_I + \frac{3x_{ci}}{\pi} I_{DC} \qquad \text{(a 18)}$$

where x_{ci} is the commutating reactance.

Combining equations (a 12), (a 17), and (a 18) the following equation can be obtained :

$$pI_{DC} = (-R_{DC} I_{DC} + \frac{3\sqrt{3}}{\pi} n v_{ds} \cos\alpha_R + \frac{3\sqrt{3}}{\pi} v_{inv} \cos\alpha_I - \frac{3x_{ci}}{\pi} I_{DC}) / L_{DC} \qquad \text{(a 19)}$$

A.4 Self Excitation Capacitor Model

Referring to the d-q equivalent circuit of the self excitation capacitor shown in Fig. (A1), the following differential equations can be written:

$$pv_{qs} = \frac{i_{qc}}{C_0} - \omega_s v_{ds} \qquad \text{(a 20)}$$

$$pv_{ds} = \frac{i_{dc}}{C_0} + \omega_s v_{qs} \qquad \text{(a 21)}$$

Since, $v_{qs} = 0$, due to the choice of axis alignment, equations (a20-a21) can be rewritten as:

$$\omega_s = \frac{i_{qc}}{C_0 v_{ds}} \qquad \text{(a 22)}$$

$$pv_{ds} = \frac{i_{dc}}{C_0} \qquad \text{(a 23)}$$

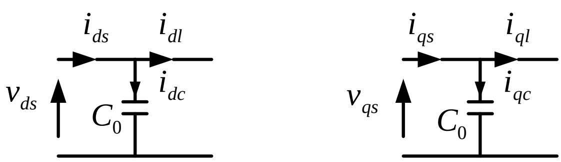

Fig. A1: d-q equivalent circuit of the self excitation capacitor.

Referring to Fig. (A1), the values of i_{qc} and i_{dc} can be written as:

$$i_{qc} = i_{qs} - i_{ql} \quad , \quad i_{dc} = i_{ds} - i_{dl} \qquad \text{(a 24)}$$

Equations (a11, a14 and a15) are combined with equation (a24) as:

$$i_{qc} = i_{qs} + \frac{2\sqrt{3}}{\pi} nI_{DC} \sin\alpha_R \quad , \quad i_{dc} = i_{ds} - \frac{2\sqrt{3}}{\pi} nI_{DC} \cos\alpha_R \qquad \text{(a 25)}$$

Substituting the values of i_{qc} and i_{dc} from equation (a 25) into equations (a 22) and (a 23) would give:

$$\omega_s = \frac{i_{qs} + \frac{2\sqrt{3}}{\pi} nI_{DC} \sin\alpha_R}{C_0 v_{ds}} \quad \text{(a 26)}$$

$$pv_{ds} = \frac{i_{ds} - \frac{2\sqrt{3}}{\pi} nI_{DC} \cos\alpha_R}{C_0} \quad \text{(a 27)}$$

Equation (a 26) can be used to determine the electrical frequency of the voltage generated by the induction generator.

A.5 Voltage Regulator Model

The DC voltage at the output of the converter terminals can be regulated by controlling the firing angle α_R as described in the following differential equation :

$$p\alpha_R = V_{ref} - V_R = V_{ref} - \frac{3\sqrt{3}}{\pi} nv_{ds} \cos\alpha_R$$

where V_{ref} is the reference voltage of the converter output.

A.6 Power Regulator Model

The power output of the converter (power delivered to the asynchronous AC-DC-AC link by the wind energy system) can be adjusted via controlling the inverter firing angle α_I according to the following differential equation:

$$p\alpha_I = P_{ref} - P = P_{ref} - (\frac{3\sqrt{3}}{\pi} nv_{ds} \cos\alpha_R) I_{DC}$$

where P_{ref} is the reference power at the output of the converter.

APPENDIX B

The elements a_{ij} of the 9 x 9 matrix A are :

$$\mathbf{a}_{11} = -\mathbf{R_s A}_1 - (\mathbf{I}_{\mathbf{ds}0} / \mathbf{C}_0 \mathbf{V}_{\mathbf{ds}0})$$

$$\mathbf{a}_{12} = -(\mathbf{I}_{\mathbf{qs}0} / \mathbf{C}_0 \mathbf{V}_{\mathbf{ds}0}) - (\frac{2\sqrt{3}\mathbf{nI}_{\mathbf{DC}0} \sin\alpha_{\mathbf{R}0}}{\pi \mathbf{C}_0 \mathbf{V}_{\mathbf{ds}0}}) - \mathbf{A}_2 \omega_{\mathbf{m}0} \mathbf{L_m}, \quad \mathbf{a}_{13} = -\mathbf{a}_{24} = -\mathbf{R_r A}_2, \quad \mathbf{a}_{14} = -\mathbf{A}_1 \omega_{\mathbf{m}0} \mathbf{L_r}$$

$$\mathbf{a}_{15} = -\mathbf{A}_2 \mathbf{L_m I}_{\mathbf{ds}0} - \mathbf{A}_1 \mathbf{L_r I}_{\mathbf{dr}0}, \quad \mathbf{a}_{16} = \frac{\mathbf{I}_{\mathbf{qs}0} + \frac{2\sqrt{3}}{\pi} \mathbf{nI}_{\mathbf{DC}0} \sin\alpha_{\mathbf{R}0}}{\mathbf{C}_0 (\mathbf{V}_{\mathbf{ds}0})^2}) - \mathbf{A}_2 \omega_{\mathbf{m}0} \mathbf{L_m}, \quad \mathbf{a}_{17} = -(\frac{2\sqrt{3}\mathbf{nI}_{\mathbf{ds}0} \sin\alpha_{\mathbf{R}0}}{\pi \mathbf{C}_0 \mathbf{V}_{\mathbf{ds}0}})$$

$$\mathbf{a}_{18} = -\left(\frac{2\sqrt{3}\mathbf{nI}_{\mathbf{dc}0}\cos\alpha_{\mathbf{R}0}}{\pi\mathbf{C}_0\mathbf{V}_{\mathbf{ds}0}}\right) , \quad \mathbf{a}_{21} = (2\mathbf{I}_{\mathbf{qs}0}/\mathbf{C}_0\mathbf{V}_{\mathbf{ds}0}) + \left(\frac{2\sqrt{3}\mathbf{nI}_{\mathbf{DC}0}\sin\alpha_{\mathbf{R}0}}{\pi\mathbf{C}_0\mathbf{V}_{\mathbf{ds}0}}\right) + \mathbf{A}_2\omega_{\mathbf{m}0}\mathbf{L}_{\mathbf{m}} , \quad \mathbf{a}_{22} = -\mathbf{R}_{\mathbf{s}}\mathbf{A}_1 ,$$

$$\mathbf{a}_{23} = -\mathbf{A}_1\omega_{\mathbf{m}0}\mathbf{L}_{\mathbf{m}}$$

$$\mathbf{a}_{25} = \mathbf{A}_2\mathbf{L}_{\mathbf{m}}\mathbf{I}_{\mathbf{qs}0} + \mathbf{A}_1\mathbf{L}_{\mathbf{m}}\mathbf{I}_{\mathbf{qr}0} , \quad \mathbf{a}_{26} = \frac{-[(\mathbf{I}_{\mathbf{qs}0})^2 + \frac{2\sqrt{3}}{\pi}\mathbf{nI}_{\mathbf{qs}0}\mathbf{I}_{\mathbf{DC}0}\sin\alpha_{\mathbf{R}0}]}{\mathbf{C}_0(\mathbf{V}_{\mathbf{ds}0})^2} - \mathbf{A}_1 , \quad \mathbf{a}_{27} = \frac{2\sqrt{3}\mathbf{nI}_{\mathbf{qs}0}\sin\alpha_{\mathbf{R}0}}{\pi\mathbf{C}_0\mathbf{V}_{\mathbf{ds}0}}$$

$$\mathbf{a}_{28} = \frac{2\sqrt{3}\mathbf{nI}_{\mathbf{DC}0}\mathbf{I}_{\mathbf{qs}0}\cos\alpha_{\mathbf{R}0}}{\pi\mathbf{C}_0\mathbf{V}_{\mathbf{ds}0}} , \quad \mathbf{a}_{31} = \mathbf{a}_{42} = \mathbf{R}_{\mathbf{s}}\mathbf{A}_2 , \quad \mathbf{a}_{32} = \mathbf{A}_2\omega_{\mathbf{m}0}\mathbf{L}_{\mathbf{s}} , \quad \mathbf{a}_{33} = \mathbf{a}_{44} = -\mathbf{R}_{\mathbf{r}}(1 + \mathbf{A}_2\mathbf{L}_{\mathbf{m}})/\mathbf{L}_{\mathbf{r}}$$

$$\mathbf{a}_{34} = -\mathbf{a}_{43} = -\frac{\mathbf{I}_{\mathbf{qs}0} + \frac{2\sqrt{3}}{\pi}\mathbf{nI}_{\mathbf{DC}0}\sin\alpha_{\mathbf{R}0}}{\mathbf{C}_0\mathbf{V}_{\mathbf{ds}0}} + \mathbf{A}_1\omega_{\mathbf{m}0}\mathbf{L}_{\mathbf{s}} , \quad \mathbf{a}_{35} = \mathbf{A}_2\mathbf{L}_{\mathbf{s}}\mathbf{I}_{\mathbf{ds}0} + \mathbf{A}_1\mathbf{L}_{\mathbf{s}}\mathbf{I}_{\mathbf{dr}0} ,$$

$$\mathbf{a}_{36} = \left(\frac{\mathbf{I}_{\mathbf{qs}0} + \frac{2\sqrt{3}}{\pi}\mathbf{nI}_{\mathbf{DC}0}\sin\alpha_{\mathbf{R}0}}{\mathbf{C}_0(\mathbf{V}_{\mathbf{ds}0})^2}\right)\mathbf{I}_{\mathbf{dr}0}$$

$$\mathbf{a}_{37} = -\frac{2\sqrt{3}\mathbf{nI}_{\mathbf{dr}0}\sin\alpha_{\mathbf{R}0}}{\pi\mathbf{C}_0\mathbf{V}_{\mathbf{ds}0}} , \quad \mathbf{a}_{38} = \frac{-2\sqrt{3}\mathbf{nI}_{\mathbf{DC}0}\mathbf{I}_{\mathbf{dr}0}\cos\alpha_{\mathbf{R}0}}{\pi\mathbf{C}_0\mathbf{V}_{\mathbf{ds}0}} , \quad \mathbf{a}_{41} = (\mathbf{I}_{\mathbf{qr}0}/\mathbf{C}_0\mathbf{V}_{\mathbf{ds}0}) - \mathbf{A}_2\omega_{\mathbf{m}0}\mathbf{L}_{\mathbf{s}}$$

$$\mathbf{a}_{45} = -\mathbf{A}_2\mathbf{L}_{\mathbf{s}}\mathbf{I}_{\mathbf{qs}0} + \mathbf{A}_1\mathbf{L}_{\mathbf{s}}\mathbf{I}_{\mathbf{qr}0} , \quad \mathbf{a}_{46} = -\left(\frac{\mathbf{I}_{\mathbf{qs}0} + \frac{2\sqrt{3}}{\pi}\mathbf{nI}_{\mathbf{DC}0}\sin\alpha_{\mathbf{R}0}}{\mathbf{C}_0(\mathbf{V}_{\mathbf{ds}0})^2}\right)\mathbf{I}_{\mathbf{qr}0} + \mathbf{A}_2 , \quad \mathbf{a}_{47} = \frac{2\sqrt{3}\mathbf{nI}_{\mathbf{qr}0}\sin\alpha_{\mathbf{R}0}}{\pi\mathbf{C}_0\mathbf{V}_{\mathbf{ds}0}}$$

$$\mathbf{a}_{48} = \frac{2\sqrt{3}\mathbf{nI}_{\mathbf{DC}0}\mathbf{I}_{\mathbf{qr}0}\cos\alpha_{\mathbf{R}0}}{\pi\mathbf{C}_0\mathbf{V}_{\mathbf{ds}0}} , \quad \mathbf{a}_{51} = 3\mathbf{P}^2\mathbf{L}_{\mathbf{m}}\mathbf{I}_{\mathbf{dr}0}/2\mathbf{J} ,$$

$$\mathbf{a}_{53} = -3\mathbf{P}^2\mathbf{L}_{\mathbf{m}}\mathbf{I}_{\mathbf{ds}0}/2\mathbf{J} , \quad \mathbf{a}_{54} = 3\mathbf{P}^2\mathbf{L}_{\mathbf{m}}\mathbf{I}_{\mathbf{qs}0}/2\mathbf{J} \quad \mathbf{a}_{55} = -\mathbf{f}/\mathbf{J} , \quad \mathbf{a}_{62} = \frac{1}{\mathbf{C}_0}$$

$$\mathbf{a}_{67} = \frac{-2\sqrt{3}\mathbf{n}\cos\alpha_{\mathbf{R}0}}{\pi\mathbf{C}_0} , \quad \mathbf{a}_{68} = \frac{2\sqrt{3}\mathbf{nI}_{\mathbf{DC}}\sin\alpha_{\mathbf{R}0}}{\pi\mathbf{C}_0} , \quad \mathbf{a}_{76} = \frac{3\sqrt{3}}{\mathbf{L}_{\mathbf{DC}}\pi}\mathbf{n}\cos\alpha_{\mathbf{R}} , \quad \mathbf{a}_{77} = \left(-\mathbf{R}_{\mathbf{DC}} - \frac{3\mathbf{x}_{\mathbf{ci}}}{\pi}\right)/\mathbf{L}_{\mathbf{DC}}$$

$$\mathbf{a}_{78} = \left(-\frac{3\sqrt{3}}{\pi}\mathbf{nV}_{\mathbf{ds}0}\sin\alpha_{\mathbf{R}0}\right)/\mathbf{L}_{\mathbf{DC}} , \quad \mathbf{a}_{79} = \left(-\frac{3\sqrt{3}}{\pi}\mathbf{nV}_{\mathbf{ds}0}\sin\alpha_{\mathbf{R}0}\right)/\mathbf{L}_{\mathbf{DC}} , \quad \mathbf{a}_{86} = \left(-\frac{3\sqrt{3}}{\pi}\mathbf{n}\cos\alpha_{\mathbf{R}0}\right) ,$$

$$\mathbf{a}_{88} = \left(\frac{3\sqrt{3}}{\pi}\mathbf{nV}_{\mathbf{ds}0}\sin\alpha_{\mathbf{R}0}\right) , \quad \mathbf{a}_{96} = \left(-\frac{3\sqrt{3}}{\pi}\mathbf{nI}_{\mathbf{DC}0}\cos\alpha_{\mathbf{R}0}\right) , \quad \mathbf{a}_{97} = \left(-\frac{3\sqrt{3}}{\pi}\mathbf{nV}_{\mathbf{ds}0}\cos\alpha_{\mathbf{R}0}\right)$$

$$\mathbf{a}_{98} = \left(\frac{3\sqrt{3}}{\pi}\mathbf{nV}_{\mathbf{ds}0}\mathbf{I}_{\mathbf{DC}0}\sin\alpha_{\mathbf{R}0}\right) , \quad \mathbf{a}_{19} = \mathbf{a}_{29} = \mathbf{a}_{39} = \mathbf{a}_{49} = \mathbf{a}_{56} = \mathbf{a}_{57} = \mathbf{a}_{58} = \mathbf{a}_{59} = \mathbf{a}_{61} = \mathbf{a}_{63} = \mathbf{a}_{64} = \mathbf{a}_{65} = \mathbf{a}_{66} = \mathbf{a}_{69} = 0$$

$$\mathbf{a}_{71} = \mathbf{a}_{72} = \mathbf{a}_{73} = \mathbf{a}_{74} = \mathbf{a}_{75} = \mathbf{a}_{81} = \mathbf{a}_{82} = \mathbf{a}_{83} = \mathbf{a}_{84} = \mathbf{a}_{85} = \mathbf{a}_{87} = \mathbf{a}_{89} = 0$$

$$\mathbf{a}_{91} = \mathbf{a}_{92} = \mathbf{a}_{93} = \mathbf{a}_{94} = \mathbf{a}_{95} = \mathbf{a}_{99} = 0 .$$

APPENDIX C : SYSTEM PARAMETERS

Wind Turbine :

Rating : 1 kw , 450 rpm (low speed side) at V_w = 12 m/s .

Size : Height = 4 m , Equator radius = 1 m , Swept area = 4 m^2 , ρ = 1.25 kg/ m^2.

Induction Machine :

Rating : 3-phase , 2 kw , 120 V , 10 A , 4-pole , 1740 rpm .

Parameters : $R_s = 0.62\ \Omega$, $R_r = 0.566\ \Omega$, $L_s = L_r = 0.058174$ H. , $L_m = 0.054$ H, $J = 0.0622$ kg.m^2 , $f = 0.00366$ N.m./rad/s.

DC Link : $R_{DC} = 1.7\ \Omega$, $L_{DC} = 0.15$ H. ,

Self Excitation Capacitor:

Rating : 176 μf / phase , 350 V , 8 A .

محكم متين مبنى على H_∞ لمولد حثي يعمل بطاقة الرياح ومتصل بالشبكة العمومية

في هذا البحث تم اقتراح استخدام محكم متين يعتمد على نظرية H_∞ للتحكم في الجهد والقدرة الناتجين من نظام توليد يعمل بطاقة الرياح. ويتكون هذا النظام من توربينه هوائية مرتبطة ميكانيكيا بمولد حثي. وتتصل أطراف المولد الحثي بالشبكة العمومية عن طريق محولي تيار ثلاثية الأطوار (موحد وعاكس) بينهما رابط تيار مستمر **(DC LINK).** ويهدف التحكم المقترح إلى تنظيم الجهد الخارج من المولد بالإضافة الي الاستفادة من الرياح بتوليد أقصى طاقة كهربية ممكنة. وهذا يتم عن طريق التحكم في زوايا إشعال عناصر الثايرستور التي يحتويها كل من محولي التيار (الموحد و العاكس).

وقد تم في هذا البحث أيضاً وصف النموذج اللاخطي للنظام المقترح وتحويله إلى خطي حول نقطة عمل محدده وتصميم المحكم **(H_∞ controller)** يعتمد على اختيار دوال وازنه **(Weighting functions)** تهدف إلى تحقيق المتانه ضد أي تغير غير محدد للنظام وكذلك تحقيق الخواص المطلوبه للنظام .

وقد تم اختبار النظام المقترح من خلال تغير جيبي وتغير فجائي في سرعة الرياح، وقد وضحت النتائج أن النظام المقترح لا يتأثر بتغير عناصر النظام أو بالأخطاء الناتجه عن القياس أو بالضوضاء المختلفه أو بالمؤثرات الخارجيه أو عدم دقه النموذج المستخدم لوصف النظام.